Electronic Supplementary Material (ESI) for Molecular Systems Design & Engineering.
This journal is © The Royal Society of Chemistry 2017

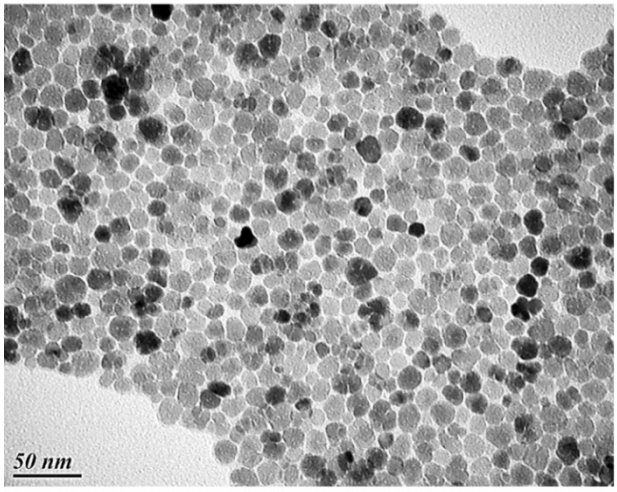

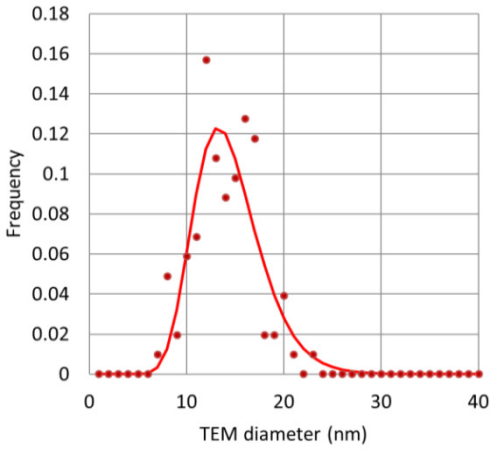

σ (nm)
3.4
d_n=<d> nm
14.45

Fig. S1. TEM micrograph and size distribution of monocore IONPs

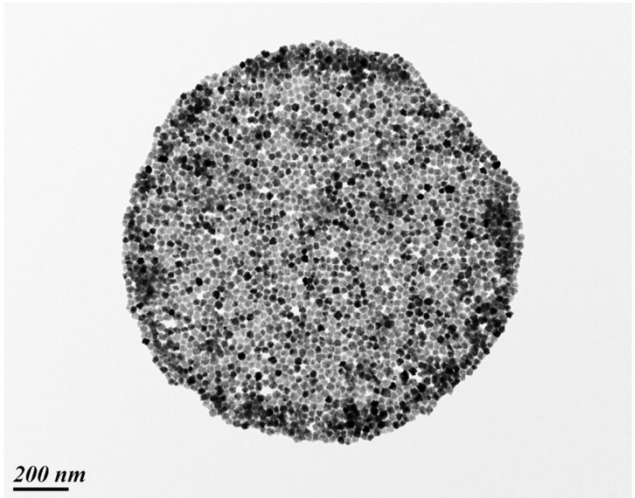

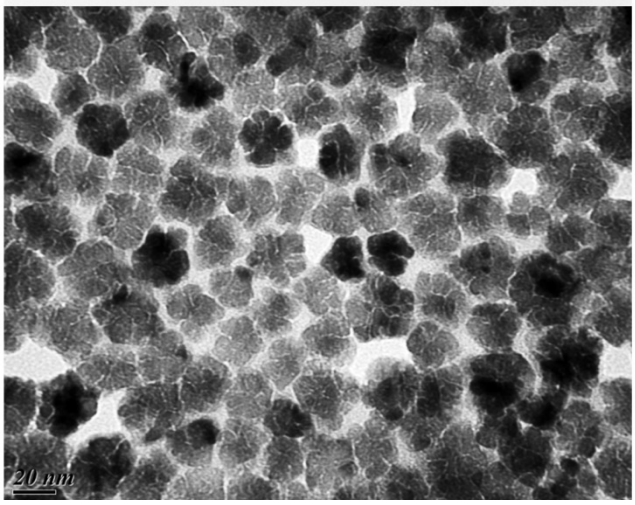

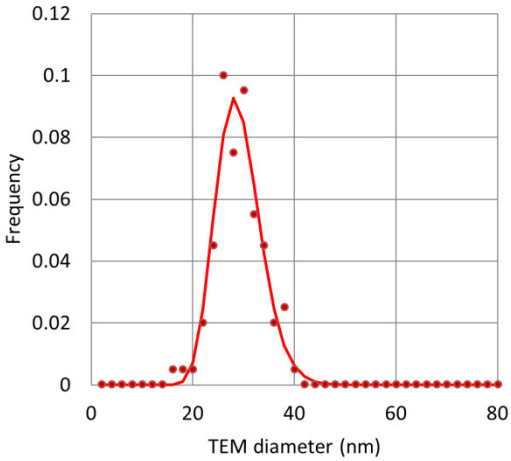

σ (nm)
4.4
d_n=<d> nm
29.1

Fig. S2. TEM micrograph and size distribution of multicore IONPs

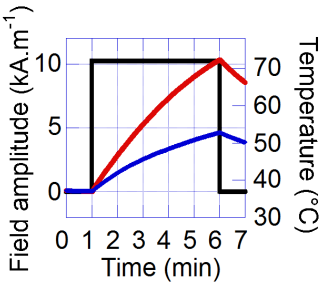

Fig. S3. Temperature increase of IONPs under an alternating magnetic field (AMF) at 755 kHz, 10.2 kA·m^{-1}, applied during 5 min, for multicore (red line) and monocore IONPs (blue line), dispersed at 3 g·L^{-1} iron oxide in dilute HNO_3 pH2. The SAR values were calculated from the initial slopes of temperature profiles within the first 5 s of AMF application. The sample tubes (1 mL) were placed in an expanded polystyrene holder for thermal insulation (yet imperfect).

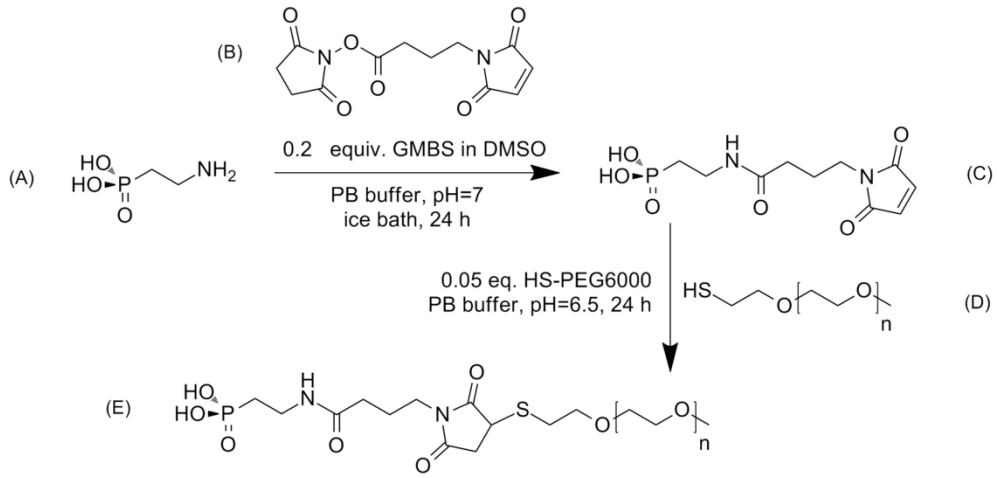

Fig. S4. Chemical modification of PEG with AEP and GMBS in order to couple it to phosphonate anchor group (AEP-GMBS-PEG).

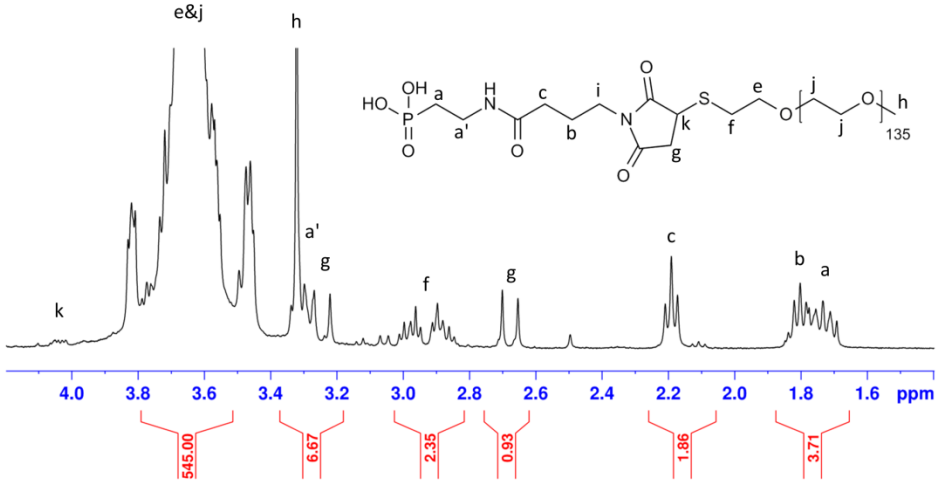

Fig. S5. ^{1}H NMR spectrum of the chemically modified AEP-GMBS-PEG in water. The peak from PEG served as a reference for the integration of other peaks, with its value fixed at 545 protons according to the average molar mass M_n=6,000 g·mol^{-1} stated by the supplier, leading to an average degree of polymerization DP=135. The reaction was quantitative for the first reaction step leading to the formation of an amide bond between GMBS and AEP. The thiol–maleimide Michael addition of PEG and AEP-GMBS had a chemical yield of 80%, possibly due to the parasitic formation of disulfides during the reaction.

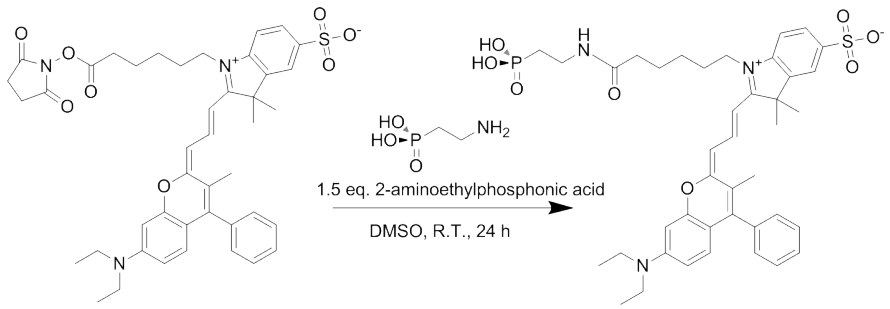

Fig. S6. Synthesis scheme of the chemical modification of the DY700-NHS fluorophore to add a phosphonic acid end-group.

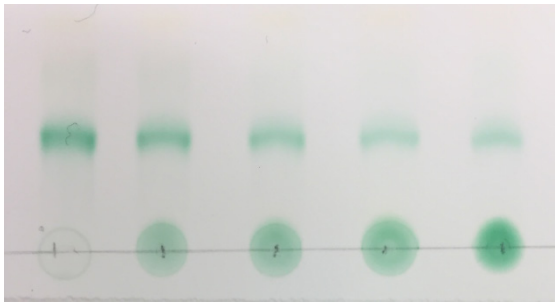

Fig. S7. 1 µL of reaction medium was spotted at regular time intervals (from left to right: 0, 1, 2.5, 4.5, and 22 h) on a thin layer chromatography (TLC) plate. The compounds were eluted using a 95:5 mixture of DCM and MeOH. Top spots correspond to DY700-NHS ester, bottom spot correspond to AEP-DY700 which phosphonate anchor group bound to the surface of silica plate. This binding effect on a metal oxide was later advantageously used to tag the surface of IONPs.

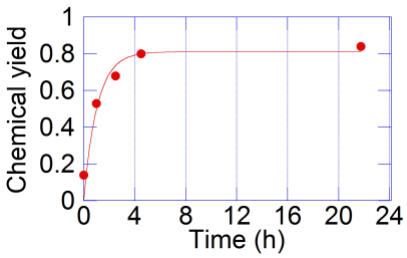

Fig. S8. Ratios of AEP-DY700/DY700 as a function of time evaluated by TLC. For this experiment, it was hypothesized that the green intensity (absorbance) was proportional to the quantity of molecules. The intensities were quantified using the gel analysis plugin in ImageJ. The green coloration in the corresponding DY700-NHS ester (top) and AEP-DY700 (bottom) areas where integrated using the ImageJ software (Fiji version https://fiji.sc/) to calculate a yield.

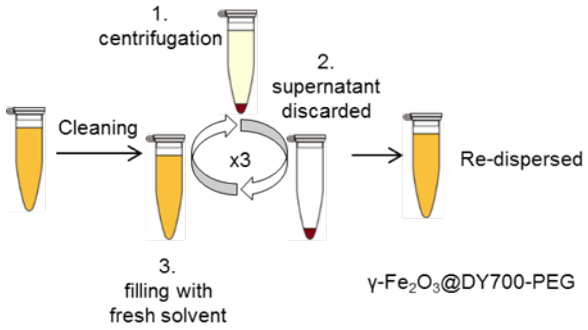

Fig. S9. Scheme of the centrifugation-redispersion process used to purify the IONPs from the excess of AEP-DY700 and AEP-GMBS-PEG. (18,000 *g*, 1 h at 25°C, 30 min at 1°C to increase viscosity and avoid pellet dispersion before removing supernatant).

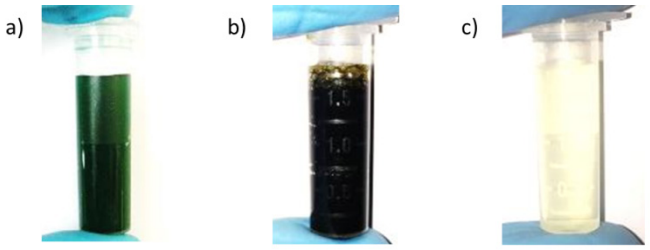

Fig. S10. a) AEP-DY700 in solution. b) Colour of the solution after addition of the IONPs and AEP-GMBS-PEG. c) Colour of the supernatant after the first round of centrifugation, showing that most of the AEP-DY700 was grafted onto the IONPs.

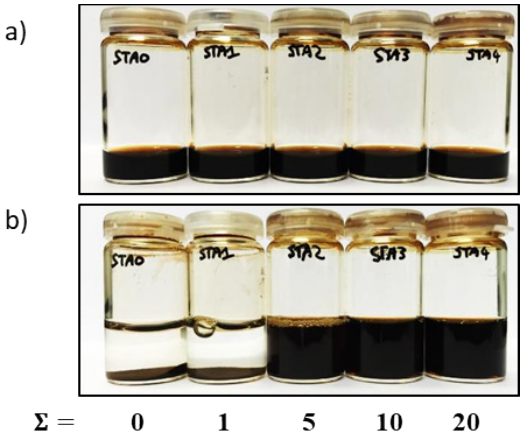

Fig. S11. Stability test of 5 samples conjugated with AEP-GMBS-PEG at various reduced tethered densities Σ **a)** before and **b)** after addition of Tris leading to a neutralization of the acidic solutions.

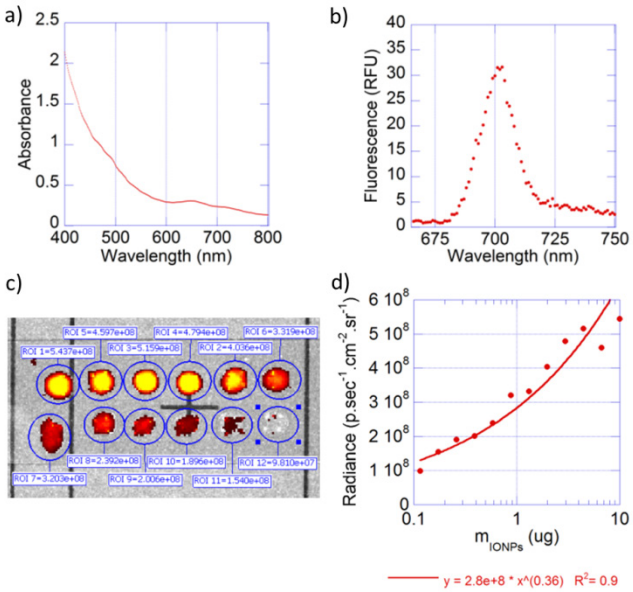

Fig. S12. a) Absorbance of multicore IONPs grafted with AEP-DY700 and AEP-GMBS-PEG. b) Fluorescence of the IONPs. c) Fluorescence of the IONPs as observed with the Lumina instrument. d) Standard calibration curve of the fluorescence intensity integrated in the circular ROIs as a function of the quantity of IONPs in each well, fitted by a power law of exponent 0.36.

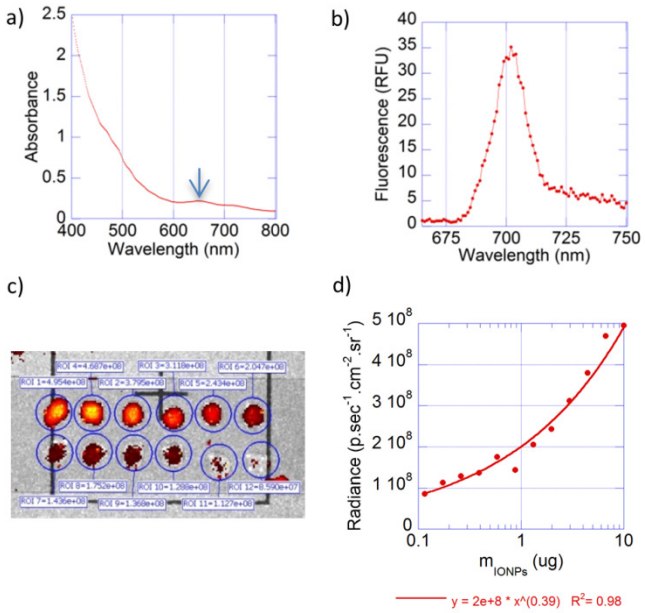

Fig. S13. a) Absorbance of monocore IONPs grafted with AEP-DY700 and AEP-GMBS-PEG. b) Fluorescence of the IONPs. c) Fluorescence of the IONPs as observed with the Lumina instrument. d) Standard calibration curve of the fluorescence intensity integrated in the circular ROIs as a function of the quantity of IONPs in each well, fitted by a power law of exponent 0.39.

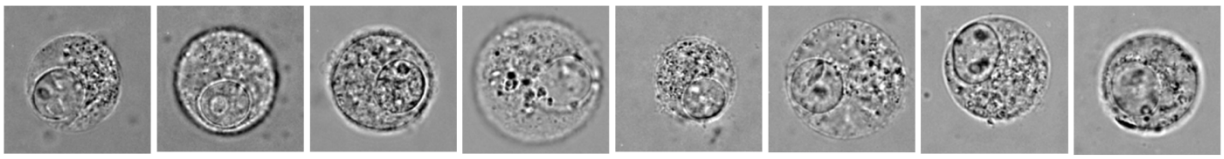

Fig. S14 Cells incubated with monocore IONPs observed by bright field microscopy showing some internal "granularity".

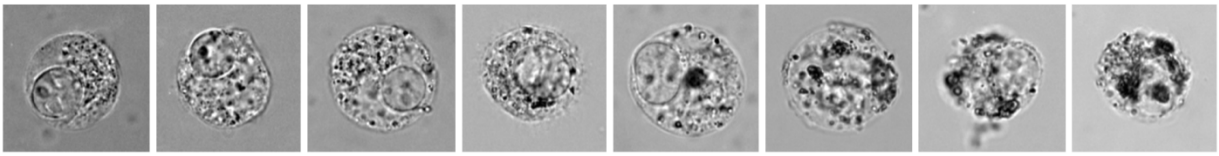

Fig. S15. Cells incubated with multicore IONPs observed by bright field microscopy, with even more dark spots inside (yet cells are perfectly alive).

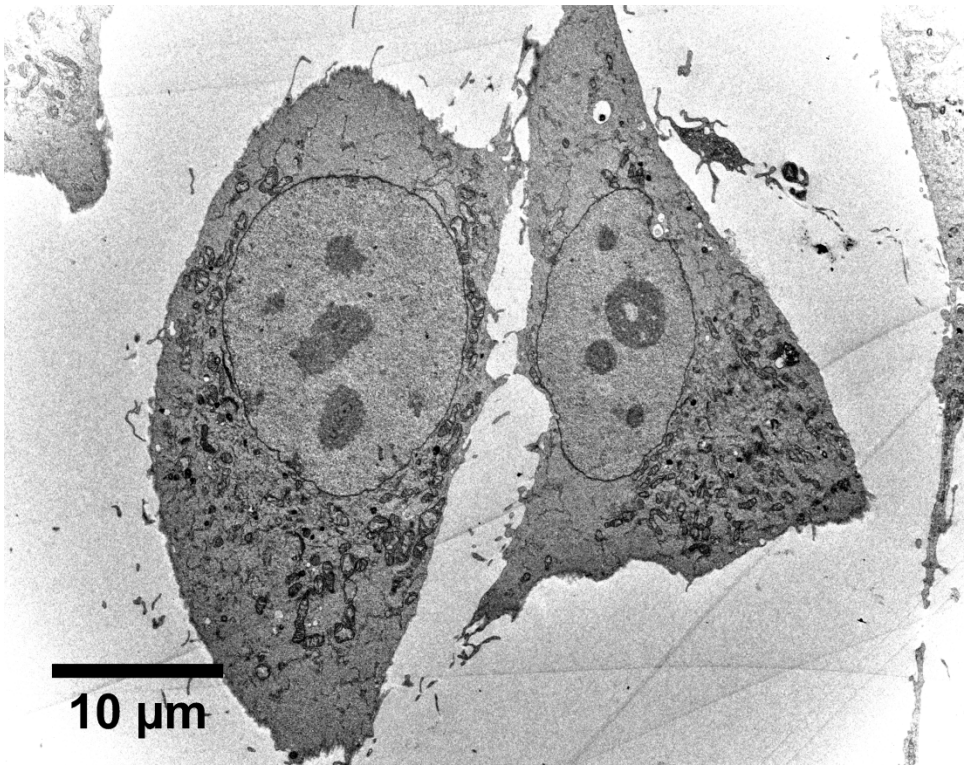

Fig. S16. U87 cells observed by TEM at low magnification, showing their microstructure.

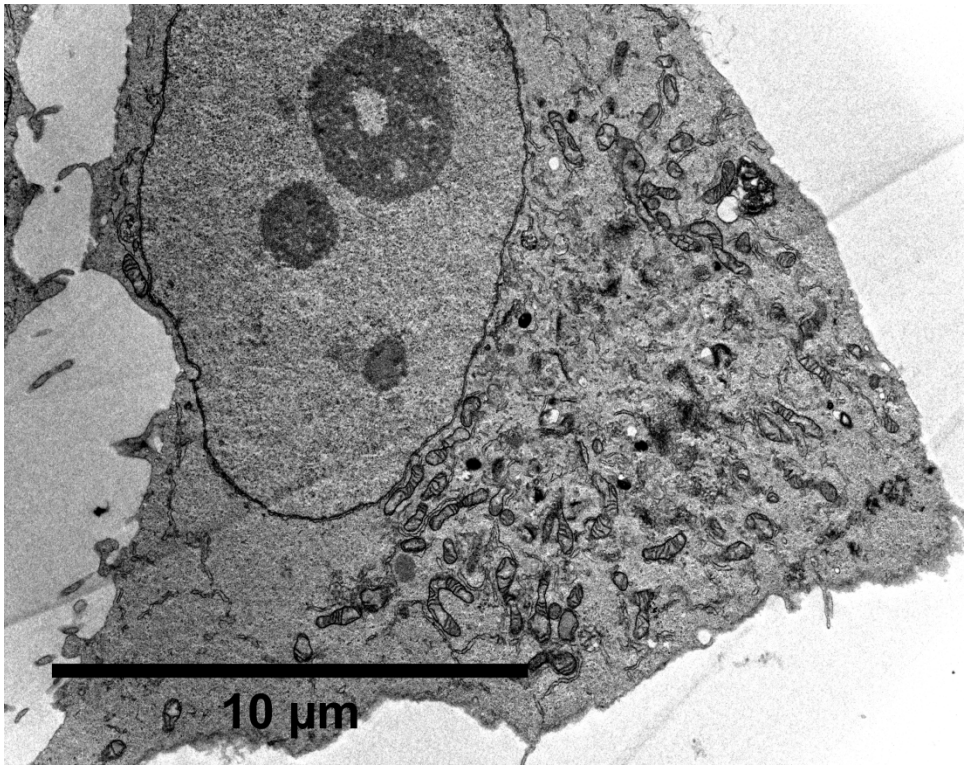

Fig. S17. U87 cells observed by TEM

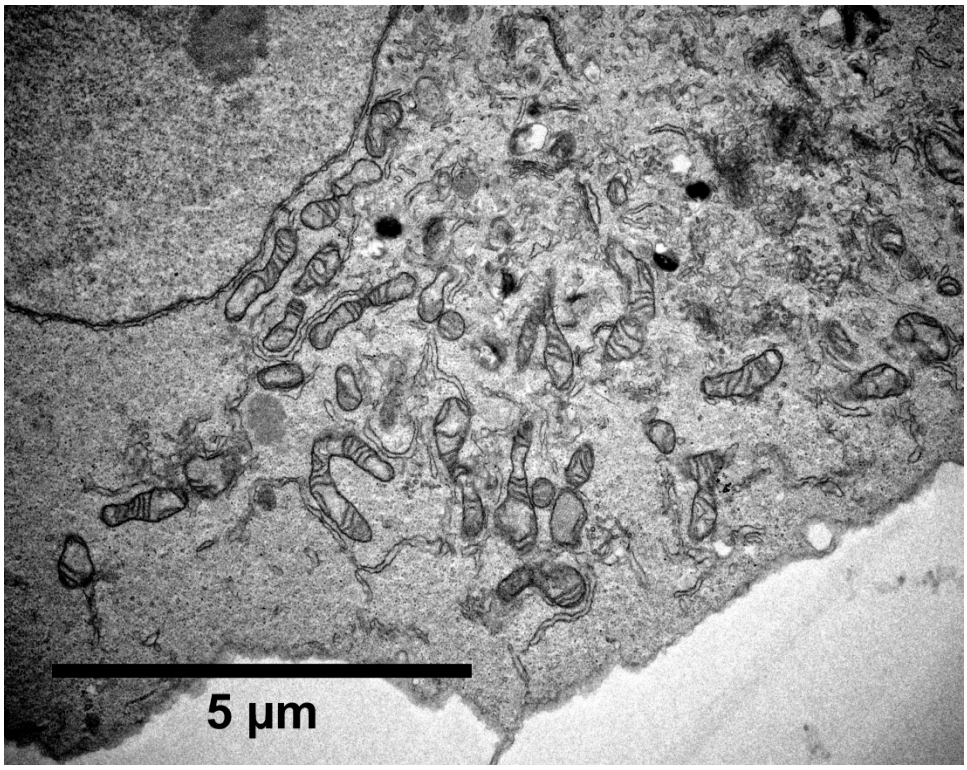

Fig. S18. U87 cells observed by TEM: Zoom on mitochondria

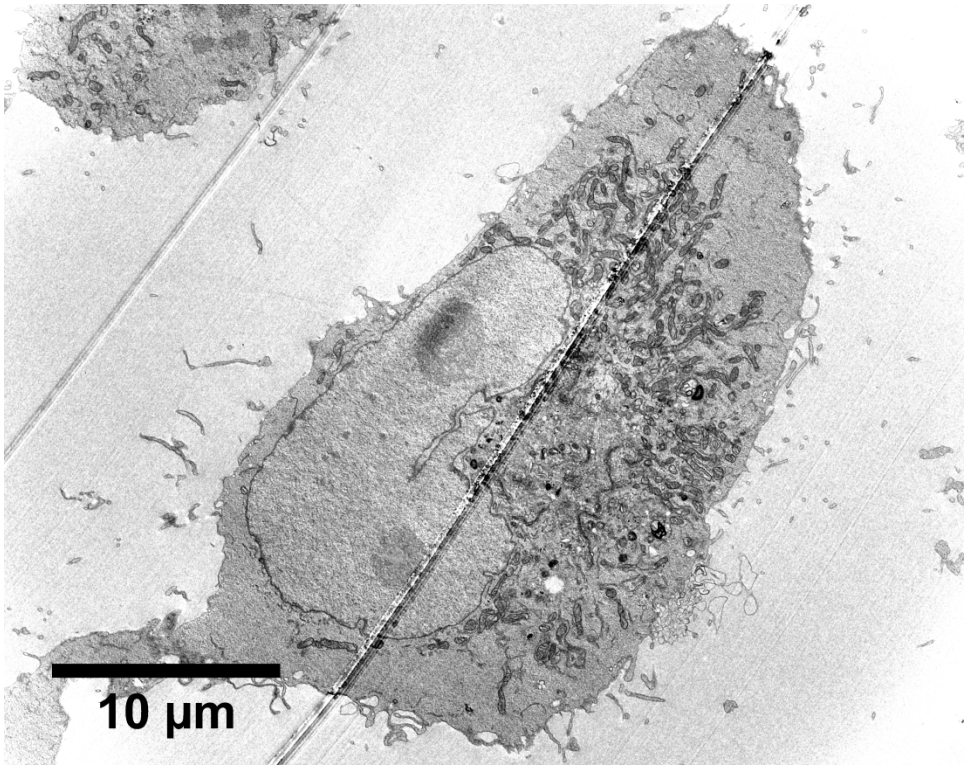

Fig. S19. U87 cells incubated with monocore IONPs observed by TEM

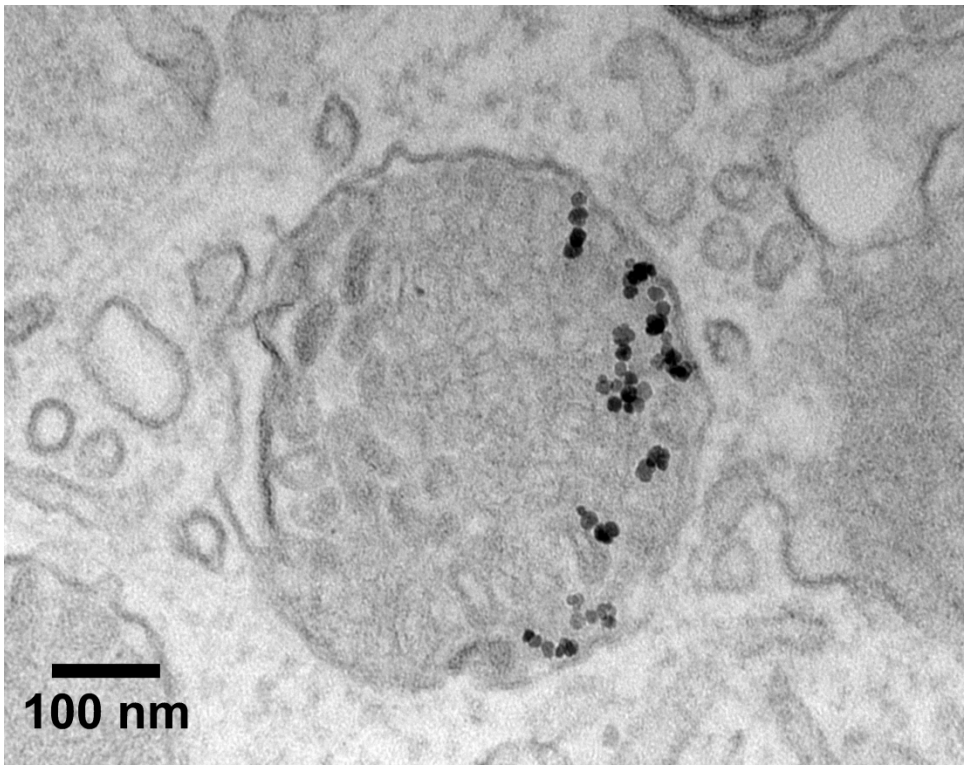

Fig. S20. U87 cells incubated with monocore IONPs observed by TEM: Zoom on a magnetic endosome

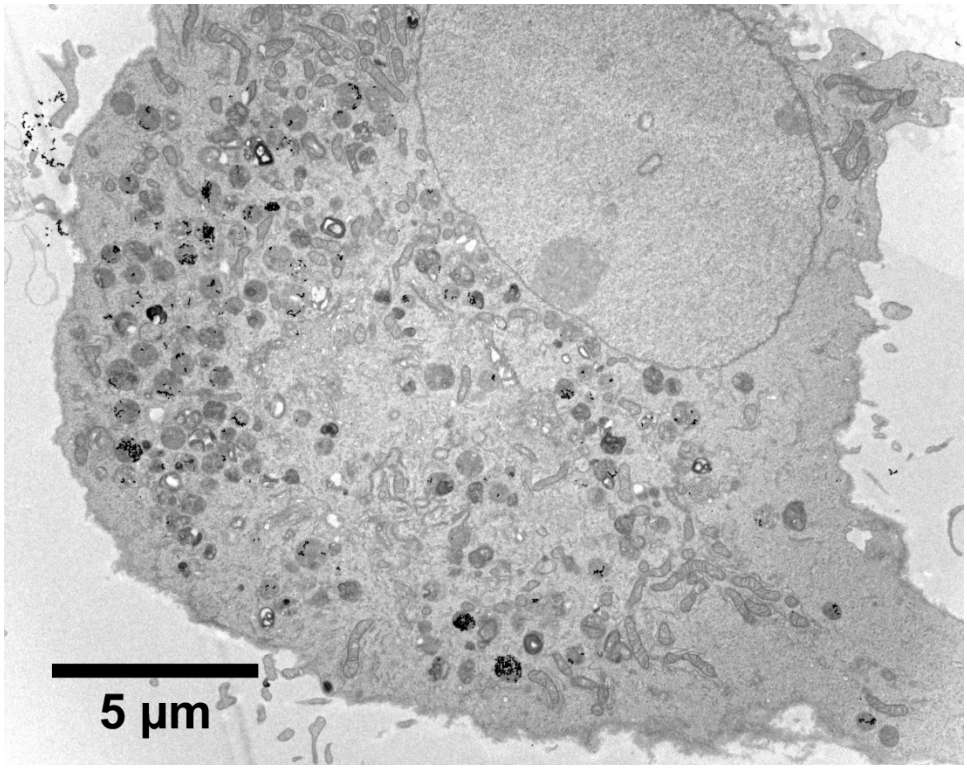

Fig. S21. U87 cells incubated with multicore IONPs observed by TEM

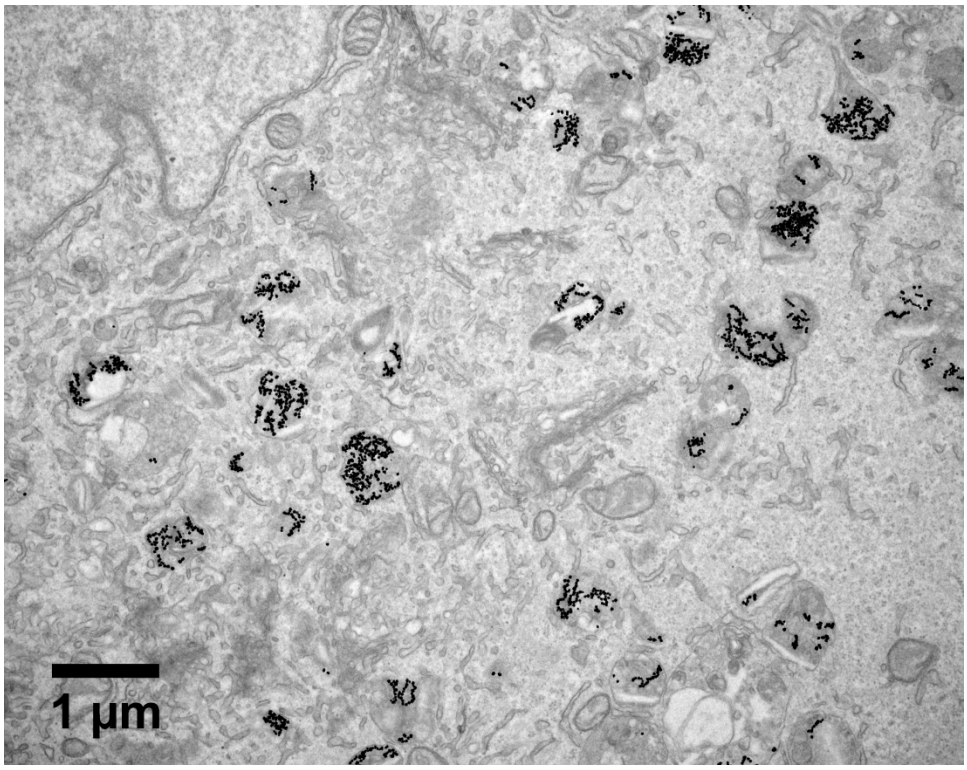

Fig. S22. U87 cells incubated with multicore IONPs observed by TEM

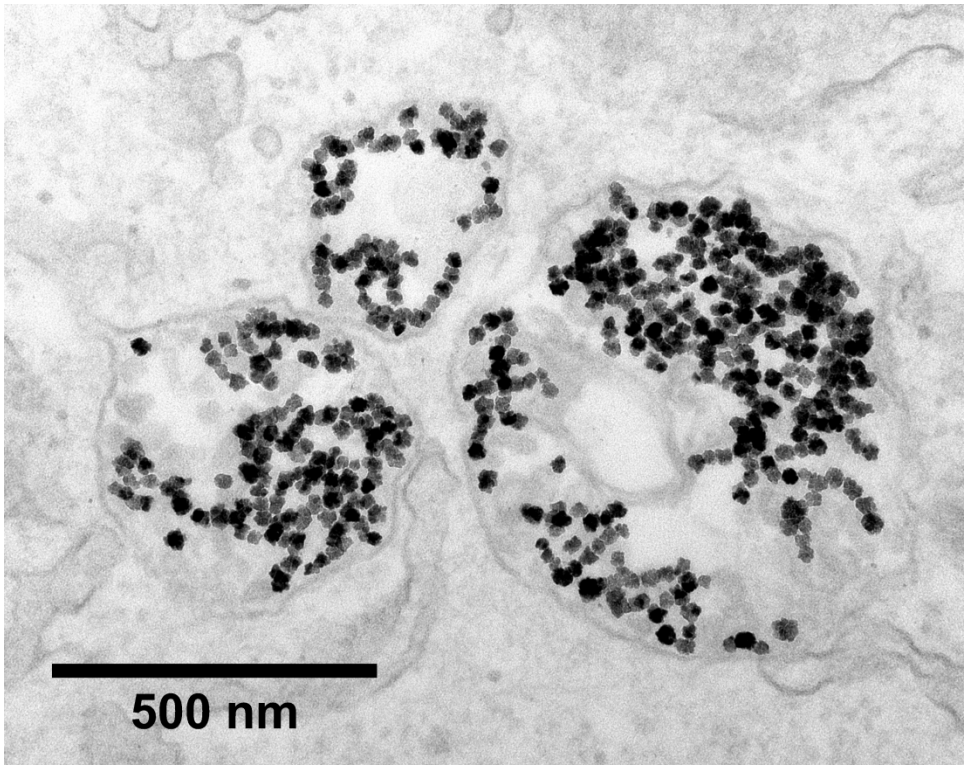

Fig. S23. U87 cells incubated with multicore IONPs observed by TEM: Zoom at high magnification of lysosomes heavily loaded in IONPs.

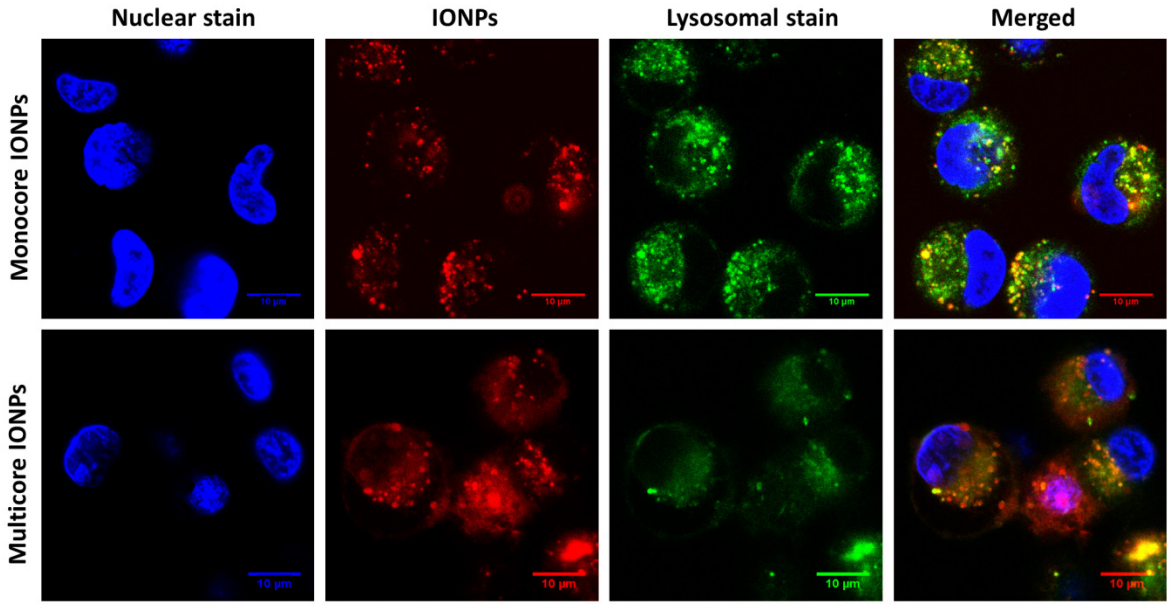

Fig. S24. Fluorescence confocal microscopy of U87 glioblastoma cells incubated with monocore or multicore IONPs. The co-localization between the red fluorescence of the IONPs (labelled with DY700 dye) and the green fluorescence of the lysosomes (labelled with Lysotracker™ dye) was quantified using the co-localization plugin of ImageJ software (https://imagej.net/Colocalization_-_hardware_setup_and_image_acquisition), yielding Pearson correlation and overlap coefficients of respectively 0.20 and 0.92 for the monocore IONPs and 0.35 and 0.94 for the multicore IONPs, showing in both case a very high co-occurrence (overlapping) yet low correlation, presumably because the green emission of Lysotracker™ is absorbed by iron oxide (thus the two signals are not proportional when the two emitting dye molecules are located within the same pixel of the image).